

Highly efficient CdS-quantum-dot-sensitized GaAs solar cells

Chien-Chung Lin,^{1*} Hsin-Chu Chen,² Yu Lin Tsai,² Hau-Vei Han,² Huai-Shiang Shih,¹
Yi-An Chang,³ Hao-Chung Kuo,² and Peichen Yu²

¹ Institute of Photonic System, College of Photonics, National Chiao-Tung University, No.301, Gaofa 3rd Rd., Guiren Dist., Tainan City 71150, Taiwan

² Department of Photonic & Institute of Electro-Optical Engineering, National Chiao Tung University, 1001 University Road, Hsinchu 30010, Taiwan

³ Millennium Communication Co., Ltd., No.2, Kuan Fu S. Rd., Hsinchu Industrial Park, Hsinchu 303, Taiwan
[*chienchunglin@faculty.nctu.edu.tw](mailto:chienchunglin@faculty.nctu.edu.tw)

Abstract: We demonstrate a hybrid design of traditional GaAs-based solar cell combined with colloidal CdS quantum dots. With anti-reflective feature at long wavelength and down-conversion at UV regime, the CdS quantum dot effectively enhance the overall power conversion efficiency by as high as 18.9% compared to traditional GaAs-based device. A more detailed study showed an increase of surface photoconductivity due to UV presence, and the fill factor of the solar cell can be improved accordingly.

©2012 Optical Society of America

OCIS codes: (040.5350) Photovoltaic; (160.4236) Nanomaterials.

References and links

1. M. A. Green, "Thin-film solar cells: review of materials, technologies and commercial status," *J. Mater. Sci. Mater. Electron.* **18**(S1), 15–19 (2007).
2. S. Siebentritt, "Wide gap chalcopyrites: material properties and solar cells," *Thin Solid Films* **403-404**, 1–8 (2002).
3. R. Klenk, J. Klaer, R. Scheer, M. C. Lux-Steiner, I. Luck, N. Meyer, and U. Rühle, "Solar cells based on CuInS₂—an overview," *Thin Solid Films* **480-481**, 509–514 (2005).
4. A. Kongkanand, K. Tvrđy, K. Takechi, M. Kuno, and P. V. Kamat, "Quantum dot solar cells. Tuning photoresponse through size and shape control of CdSe-TiO₂ architecture," *J. Am. Chem. Soc.* **130**(12), 4007–4015 (2008).
5. S. D. Standridge, G. C. Schatz, and J. T. Hupp, "Distance dependence of plasmon-enhanced photocurrent in dye-sensitized solar cells," *J. Am. Chem. Soc.* **131**(24), 8407–8409 (2009).
6. Q. Zhang, T. P. Chou, B. Russo, S. A. Jenekhe, and G. Cao, "Polydisperse aggregates of ZnO nanocrystallites: a method for energy-conversion-efficiency enhancement in dye-sensitized solar cells," *Adv. Funct. Mater.* **18**(11), 1654–1660 (2008).
7. K. Tanabe, "A review of ultrahigh efficiency III-V semiconductor compound solar cells: multijunction tandem, lower dimensional, photonic up/down conversion and plasmonic nanometallic structures," *Energies* **2**(3), 504–530 (2009).
8. C. Baur, A. Bett, F. Dimroth, G. Siefer, M. Meusel, W. Bensch, W. Kostler, and G. Strobl, "Triple-junction III-V based concentrator solar cells: perspectives and challenges," *J. Sol. Energy Eng.* **129**(3), 258–265 (2007).
9. T. Takamoto, E. Ikeda, H. Kurita, and M. Ohmori, "Over 30% efficient InGaP/GaAs tandem solar cells," *Appl. Phys. Lett.* **70**(3), 381–383 (1997).
10. W. Guter, J. Schone, S. P. Philipps, M. Steiner, G. Siefer, A. Wekkeli, E. Welsler, E. Oliva, A. W. Bett, and F. Dimroth, "Current-matched triple-junction solar cell reaching 41.1% conversion efficiency under concentrated sunlight," *Appl. Phys. Lett.* **94**(22), 223504 (2009).
11. P. Yu, C. H. Chang, C. H. Chiu, C. S. Yang, J. C. Yu, H. C. Kuo, S. H. Hsu, and Y. C. Chang, "Efficiency enhancement of GaAs photovoltaics employing antireflective indium tin oxide nanocolumns," *Adv. Mater. (Deerfield Beach Fla.)* **21**(16), 1618–1621 (2009).
12. W. Shockley and H. J. Queisser, "Detailed balance limit of efficiency of p-n junction solar cells," *J. Appl. Phys.* **32**(3), 510–519 (1961).
13. S. Geyer, V. J. Porter, J. E. Halpert, T. S. Mentzel, M. A. Kastner, and M. G. Bawendi, "Charge transport in mixed CdSe and CdTe colloidal nanocrystal films," *Phys. Rev. B* **82**(15), 155201 (2010).
14. X. Wang, G. I. Koleilat, J. Tang, H. Liu, I. J. Kramer, R. Debnath, L. Brzozowski, D. A. R. Barkhouse, L. Levina, S. Hoogland, and E. H. Sargent, "Tandem colloidal quantum dot solar cells employing a graded recombination layer," *Nat. Photonics* **5**(8), 480–484 (2011).
15. M. M. Caldwell, "Plant life and ultraviolet radiation: some perspective in the history of the earth's UV climate," *Bioscience* **29**(9), 520–525 (1979).

16. Q. Sun, Y. A. Wang, L. S. Li, D. Wang, T. Zhu, J. Xu, C. Yang, and Y. Li, "Bright, multicoloured light-emitting diodes based on quantum dots," *Nat. Photonics* **1**(12), 717–722 (2007).
17. T. Trupke, M. A. Green, and P. Würfel, "Improving solar cell efficiencies by down-conversion of high-energy photons," *J. Appl. Phys.* **92**(3), 1668–1674 (2002).
18. H.-C. Chen, C.-C. Lin, H.-W. Han, Y.-L. Tsai, C.-H. Chang, H.-W. Wang, M.-A. Tsai, H.-C. Kuo, and P. Yu, "Enhanced efficiency for c-Si solar cell with nanopillar array via quantum dots layers," *Opt. Express* **19**(S5 Suppl 5), A1141–A1147 (2011).
19. E. Klampaftis, D. Ross, K. R. McIntosh, and B. S. Richards, "Enhancing the performance of solar cells via luminescent down-shifting of the incident spectrum: a review," *Sol. Energy Mater. Sol. Cells* **93**(8), 1182–1194 (2009).
20. E. Klampaftis and B. S. Richards, "Improvement in multi-crystalline silicon solar cell efficiency via addition of luminescent material to EVA encapsulation layer," *Prog. Photovolt. Res. Appl.* **19**(3), 345–351 (2011).
21. C. Strümpel, M. McCann, G. Beaucarne, V. Arkhipov, A. Slaoui, V. C. Švrcek, C. del Cañizo, and I. Tobias, "Modifying the solar spectrum to enhance silicon solar cell efficiency—An overview of available materials," *Sol. Energy Mater. Sol. Cells* **91**(4), 238–249 (2007).
22. X. Pi, Q. Li, D. Li, and D. Yang, "Spin-coating silicon-quantum-dot ink to improve solar cell efficiency," *Sol. Energy Mater. Sol. Cells* **95**(10), 2941–2945 (2011).
23. E. Mutlugun, I. M. Soganci, and H. V. Demir, "Nanocrystal hybridized scintillators for enhanced detection and imaging on Si platforms in UV," *Opt. Express* **15**(3), 1128–1134 (2007).
24. S. M. Sze, *Physics of Semiconductor Devices* (Wiley, 2nd Edition, 1981), Chap. 14.
25. C. A. Leatherdale, C. R. Kagan, N. Y. Morgan, S. A. Empedocles, M. A. Kastner, and M. G. Bawendi, "Photoconductivity in CdSe quantum dot solids," *Phys. Rev. B* **62**(4), 2669–2680 (2000).

1. Introduction

There have been tremendous efforts to develop new green technologies to alleviate the global warming and energy crisis. Among them, novel photovoltaic materials and devices are especially important since solar cell can be integrated into our daily life easily and thus make more impacts towards energy saving. How to provide an effective way to convert solar energy into electricity is thus an important scientific issue. Since the invention of the solar cells in the 1950's, many methods and device architectures have been proposed and realized either in the lab or commercially, such as crystalline/amorphous Si-solar cell [1], chalcopyrites [2, 3], dye-/quantum-dot-sensitized solar cells [4–6] and single-/multi-junction III-V solar cells [7–9] etc. While most of these solar cell technologies provide satisfactory results, it is III-V materials that claimed the highest power conversion efficiency (PCE) so far [10, 11]. Meanwhile, the detailed-balance Shockley-Queisser limit (SQ limit) [12] puts an upper limit of 44% for the cell with single band gap material, which is yet to be conquered.

Other than semiconductor bulk or epitaxial materials, there has been a long history of utilizing colloidal quantum dots (or nanocrystals) as the active layers in solar cells. The benefits of adapting quantum dot material in the solar cell are mainly for low-cost, large area, flexible substrates and potentially high efficiency. Many extraordinary works were reported for light detection [13], tandem solar cells [14] etc. However, most of the results were limited to 10% PCE or less. How to combine both the versatility of the quantum dot material and the high PCE in semiconductor device becomes an interesting topic to research. One of the major limits in current solar cell is the lack of absorbing material at ultraviolet (UV) region. These high energy photons get absorbed quickly in the bulk material but the carriers are consumed near the surface by the traps and defects. This portion of sunlight takes up to 7% of the overall energy [15], and this percentage is even higher in the outer space. Therefore, efficient use of UV part of the solar spectrum for energy conversion is crucial. If UV photons can be harvested, it is then possible to approach the aforementioned SQ limit. One possible solution is to utilize semiconductor based quantum dots (QDs) such as CdS, CdSe, in the regular solar cell. These nano-scale materials have strong UV absorption and efficient visible down-conversion [16]. If the down-converted photons can be properly collected by the host material underneath, the UV photons can then be counted as effective as other longer wavelength ones. Theoretically, if we have 100% down-conversion efficiency and these converted photons can be completely absorbed and transferred into electrical carriers, another 7% of overall energy can be added to the present III-V solar cell [15]. This 7% belong to the aforementioned solar UV spectrum and is not related to other effects such as anti-reflection. The cell itself is still subject to the SQ limit, but the practical PCE upper limit can be raised with this down-

conversion. Previous works [17–23] have demonstrated that it is possible to use colloidal quantum dots (CQDs) or other substances (such as dye) to promote the efficiency of Si-based solar cells, either by anti-reflective (AR) effect due to the gradient refractive index introduced by the film or by the down-conversion transition of the CQDs. However, most of the results focused on silicon devices, and we are still short of an experiment on the direct band gap material. Such test can be used for a good comparison of the quantum dot effect between the direct/indirect band gap materials. In this work, we demonstrate a strong efficiency-enhanced photovoltaic response due to the introduction of CdS quantum dots on the GaAs device surface. The physics behind this phenomenon can be investigated by the solar simulator, quantum efficiency measurements, and the increase of surface charges at the presence of the quantum dots can be further proved by a pure UV excitation.

2. Experiment and device design

The single-junction p + -n GaAs solar cell structures were grown by the low pressure (50 torr) metal-organic chemical vapor deposition in a vertical reactor (Veeco D180). A Si-doped n-type GaAs substrate (100) off zero degree was used for the deposition. Trimethyl (TM-) sources of aluminum, gallium, and indium were used for group-III precursors, while arsine and phosphine were used as the group V reaction agents. Silane (SiH_4) and diethylzinc (DEZn) were used as the n-type and p-type dopant sources, respectively. The growth rate for all arsine based layers was kept at $2.0 \mu\text{m/h}$, while the indium source was precisely controlled by an Epison controller system. The V/III ratio was kept at 200 for a growth temperature range of $600\text{--}720 \text{ }^\circ\text{C}$ in this work. The uniformity of bulk layer thickness during the epitaxial growth was maintained to a less than 0.4% standard deviation in a 3-inch wafer. The epitaxial growth started from depositing a 300-nm-thick n + -GaAs buffer layer, followed by a 100-nm-thick n + - $\text{Al}_{0.3}\text{Ga}_{0.7}\text{As}$ back-surface-field layer, and a 3.5- μm -thick n-GaAs base layer. The emitter layer is a 500-nm p + -GaAs, capped by a p + - $\text{Al}_{0.8}\text{Ga}_{0.2}\text{As}$ window layer. Finally, the solar cell structures were completed by capping a 300-nm-thick p + -GaAs contact layer. After epitaxy, the fabrication processes, including photo-lithography, chemical etching, and metallization, were taken so as to fabricate the solar cell devices. In this study, back-side n-contact metal was formed by evaporating AuGe (250 Å)/Au (5000 Å), while the front p-contact was consisted of evaporated Ti (250 Å)/Pt (250 Å)/Au (5000 Å). The shadow loss of the front strip contacts is 3.5%, and area of the cells is 1 cm^2 . After the device was finished, three different samples were prepared for comparison: the first one is a clean and uncoated GaAs cell with colloidal CdS QDs with a concentration of 0.5 mg/mL spun on the surface, denoted as GaAs I. The second sample is the GaAs cell with clean surface and no AR coating, denoted as GaAs II. The third sample is the GaAs cell with AR coating centered on 670nm, named as GaAs III. A schematic plot of the finished single-junction GaAs solar cells with CdS QDs was shown in Fig. 1. The quantum dots that were used in our experiments were CdS nano-crystal produced by Sigma-Aldrich Corporation with an average size of 5 nm in diameter. In the GaAs I samples, we also took the cross-sectional TEM picture (Fig. 2), which shows multiple layers of quantum dots stacking on the surface of the device. After the device was finished, we went through the regular solar simulator test and external quantum efficiency measurement for basic device performance. The conductive atomic force microscope (CAFM), which would be used for surface photoconductivity, was performed in a Veeco Dimension 3100 Scanning Probe Microscope (D3100).

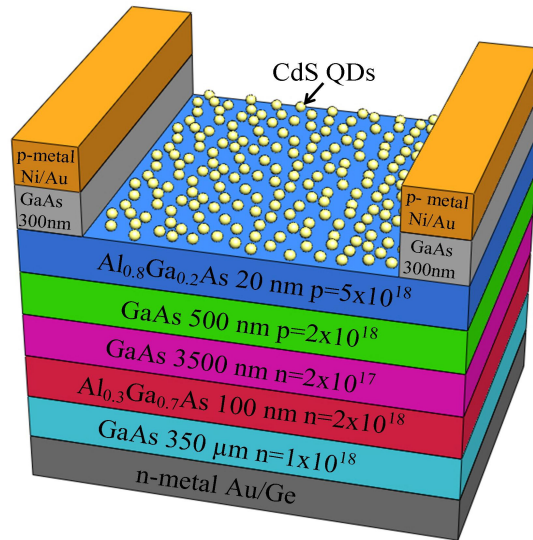


Fig. 1. A schematic plot of the fabricated single-junction GaAs solar cell with CdS QDs.

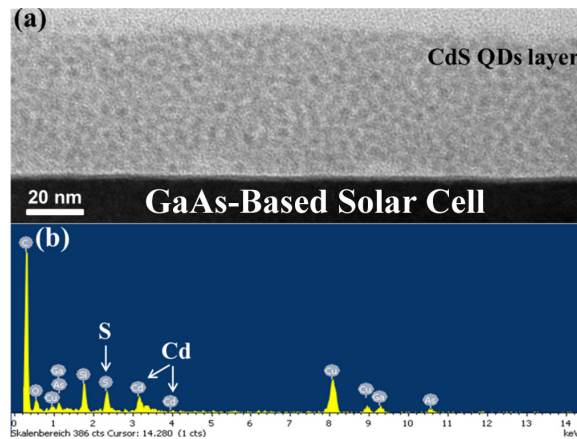


Fig. 2. (a) TEM of CdS nanocrystal on a GaAs solar cell; (b) the energy dispersive spectrometer (EDS) was taken by a JEOL JEM-2100F system.

3. Device results and discussion

Figure 3(a) shows the absorbance and photoluminescence spectrums of CdS QDs in toluene. The photoluminescence spectrum was measured by the 365 nm excitation, and a major emission peak at 460 nm was found. In absorbance spectrum, a sharp rising edge was detected around 450nm and a steady increase from 400 nm on. Therefore, this CdS QD layer is capable of converting ultraviolet photons ($\lambda < 400\text{nm}$) to the visible blue band. On the other hand, when applied to GaAs surface, even as thin as several tens of nanometer, due to its intermediate refractive index ($n \sim 2.4$), a global reduction in reflectance spectrum compared to bare semiconductor surface (as in Fig. 3(b)) was observed. The CQD layer is certainly not as good as the regular anti-reflective (AR) coating in longer wavelength but its low reflectance in shorter wavelength is impressive.

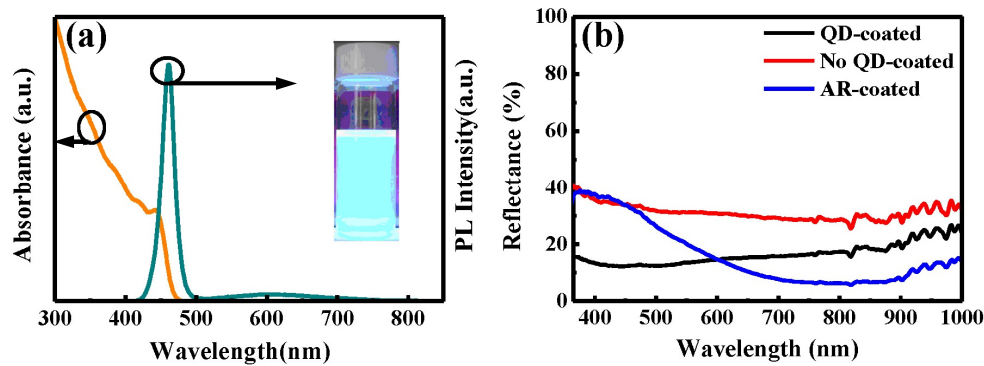


Fig. 3. (a) UV-Visible absorbance (red) and photoluminescence (blue) spectra of CdS QDs measure in toluene. The PLE spectrum was taken at the maximum of PL intensity (~470 nm). For the PL spectrum, the sample was excited by a light beam with 365 nm. The inset is the CdS quantum dot solution under UV excitation. (b) The measured reflectance spectra for QD-coated, No-QD coated, and AR-coated solar cells.

Next, the basic parameters of these devices were characterized by photovoltaic I-V curves and external quantum efficiency (EQE) measurement. The photovoltaic I-V characteristics were measured under air mass 1.5 global illumination and room temperature conditions by a class-A solar simulator complying with the IEC 904-9 standard. The results of three different types of GaAs solar cells were shown in Fig. 4. The important device parameters are summarized in Table 1. The short-circuit current density (J_{sc}) of the GaAs I (GaAs + CQDs) can reach 26.99 mA/cm^2 and its power conversion efficiency increases from 17.71% to 21.06%, corresponding to a 18.9% enhancement compared to the device without AR coating (GaAs II). When compared with the optimal AR coated device (GaAs III), the GaAs I sample still edges out by 4.1% increase in J_{sc} and 2.7% enhancement in overall power conversion efficiency. Additionally, open-circuit voltages (V_{oc}) of these devices show no degradation, and the change in fill-factor (FF) is negligible.

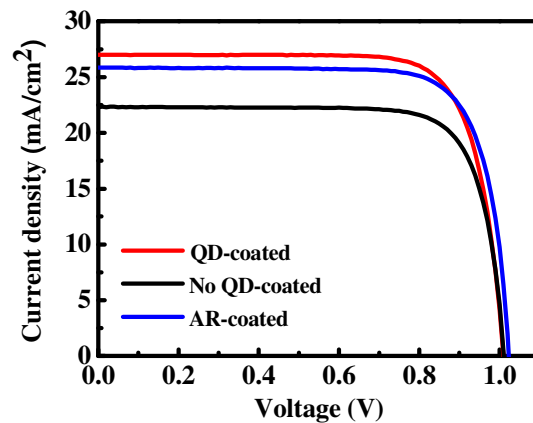


Fig. 4. Photovoltaic I-V characteristics of QD-coated, No-QD coated, and AR-coated solar cells.

Table 1. A Summarized Current-Voltage Characteristics of GaAs I, GaAs II, and GaAs III Solar Cells

Type	V_{oc} (V)	J_{sc} (mA/cm ²)	FF (%)	η (%)
GaAs w/o AR + CdS QD (GaAs I)	1.01	26.99	77.24	21.06
GaAs w/o AR (GaAs II)	1.01	22.31	78.49	17.71
GaAs with AR (GaAs III)	1.02	25.92	77.58	20.51

To further understand the utilization efficiency of photons with different wavelengths, the spectral response of the EQE was taken, and a xenon light source is used as the illumination source. Figure 5(a) shows the EQE as function of illumination wavelength for all three types of samples, and Fig. 5(b) shows the EQE enhancement factor of the GaAs I, compared to GaAs II. From EQE spectrum, the universal enhancement of GaAs I against GaAs II is exhibited, and the curves of GaAs I and GaAs III crisscross at 600nm. While the differences of EQE between CQD-coated and non-CQD-coated GaAs devices maximize at 520nm range, the ratio ($EQE_{GaAs\ I}/EQE_{GaAs\ II}$) grows rapidly once moved into ultraviolet regime ($\lambda < 350$ nm), and can be as high as 1.75 times. This result demonstrates an efficient down-conversion can subsidize the UV-generated carrier collection probability. In this scenario, the UV photons can be absorbed by CQD layer and re-emitted blue photons can be absorbed and converted much better in the bulk GaAs.

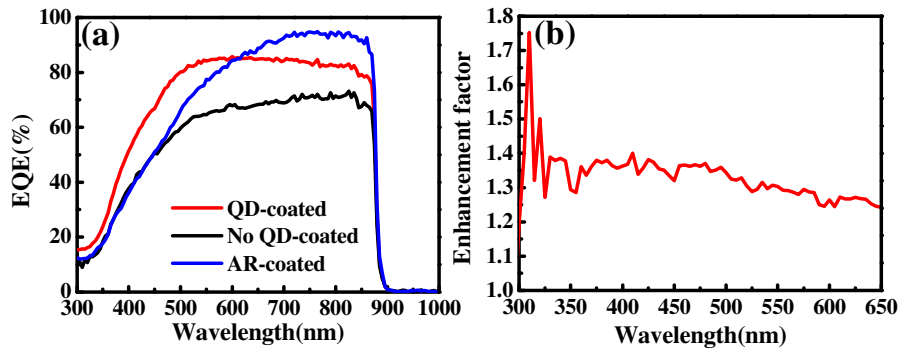


Fig. 5. (a) Measurement of External quantum efficiency of QD-coated, No-QD coated, and AR-coated solar cells. (b) Enhancement of EQE between QD-coated and No-QD coated devices. Peak at ~310 nm indicates photon down-conversion.

The contribution of the quantum dot down-conversion can be calculated by the following expression [18, 24]:

$$J_{sc} = \frac{e}{hc} \int \lambda \times EQE(\lambda) \times I_{AM1.5G}(\lambda) d\lambda \quad (1)$$

where J_{sc} is the short-circuit current, λ is the photon wavelength, $I_{AM1.5G}$ is the intensity of the AM1.5G solar spectrum. We can further calculate the percentage that comes from quantum dot down-conversion. Ideally the photons shorter than 450nm are counted as the down-converted ones, and we use the above equation to identify that there are about 11% of enhancement of short-circuit current coming from this down-conversion.

To understand more on UV response of the CQD coated devices, a UV lamp was used as the light source to test their IV under the excitation with higher photon energies. Even though our UV lamp is not standard, the enhancement of J_{sc} is quite clear in Fig. 6. When a bandpass filter (at 380nm, FWHM is 10nm) was placed to further reduce the number of low-energy photons, a rising trend of efficiency versus filtered power was observed in Fig. 6, and a constant efficiency enhancement factor of 1.22 times to the no-CQD sample was measured. Another interesting feature that is not seen in previous shown good device is the improvement

of the fill factor (FF). For a device with a bad FF as in Fig. 6, adding CQD layer on its semiconductor surface modify its photoconductivity dramatically [25] and the FF becomes much better. The increment can be as large as 30% (from 57% to 74%). In addition to macroscopic IV measurement, conductive AFM is another tool for microscopic analysis. In the normal CAFM measurement, a fixed voltage (5V) is applied on the tip of the probe, and the current is drawn from the surface atoms. A UV lamp was added during the measurement and with the lamp going on and off, the shift of surface current distribution was detected as in Fig. 7. The increase of current due to UV excitation can be found as high as 76%, if the mean detected current of each group is put to comparison. This is a clear indication of surface charges activation during the UV illumination.

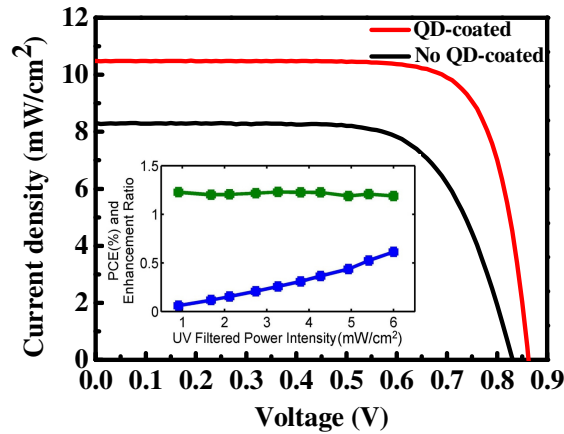


Fig. 6. IV Measurement with UV light. The inset is the filtered UV PCE of the CQD/GaAs cell (blue line) and the efficiency enhancement ($\eta_{\text{CQD}}/\eta_{\text{no CQD}}$, green line).

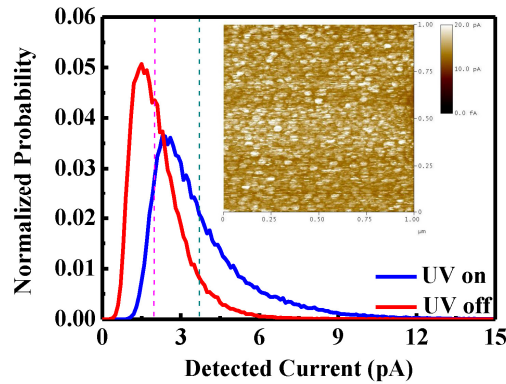


Fig. 7. The distribution of detected currents of QD on GaAs surface with and without UV lamp on. The pink and blue vertical lines indicate the average currents from the measurement. When UV lamp is off, the average current is 2.10pA. If we turn on the UV lamp, the average jump up to 3.69pA (an 76% increase). The inset is the conductive AFM scanning plot.

From these experiments, the introduction of CdS quantum dots on semiconductor surface could bring several advantages: first is the aforementioned down-conversion and anti-reflection; second is the population increase of electronic carriers at the surface because of UV excitation. Both effects can greatly improve the EQE (optical) and fill factor (electrical) of our traditional GaAs-based solar cells. One of the benefits that we did not examine in this article is the removable feature of these quantum dot layers. Once the quantum dots are degraded because of air exposure, they can be washed out by proper solvent and re-coat the

device with another fresh quantum dot material. With this way, the device can be relieved of the reliability concerns that usually accompany with these quantum dots.

So far, our analysis is based on observation of individual experiments and dividing the improvement between down-conversion and anti-reflection effect. However, the nature of this hybrid design is more complicated than this ideal scenario. Especially when the anti-reflection effect intertwine with the down-conversion, and how to properly estimate the effectiveness of down-conversion becomes difficult. In our case, several tests were performed for quantum-dot only transmission, reflection and absorption. What we found is about 10% of the UV photons can be absorbed in a single pass through the quantum dots. Combining with the reflection data in Fig. 3(b) and the EQE data, approximately 50% of the short-circuit current enhancement in UV region can be attributed to down-conversion. The previous calculated numbers (11%) of Eq. (1) based on ideal case has to be cut in half. The quantum yield of the quantum dots is assumed to be 50% to 60%. If the yield can be raised, the down-conversion can take a larger part of J_{sc} enhancement.

Another issue raised is the emission wavelength of our quantum dots. Since 460nm is not particularly favorable in photo-generated carrier collection, longer wavelength quantum dots should be considered. However, if the direct band gap material is used, the absorption edge of the QD will be very close to the emission peak, and a large portion of visible spectrum becomes absorptive to the QD. Since the overall photo-generated carriers can be expressed as the summation of carriers generated by bulk and by down-converted photons, and the quantum efficiency of the bulk material is still much higher than that of the down-conversion, the overall power conversion efficiency is expected to drop. So if we are going to use the direct band gap quantum dots, staying at shorter wavelength should be a better choice. Another solution will be the indirect band gap material such as silicon. The indirect band gap material can have a much larger Stoke shift between the absorption edge and emission peak. We believe this indirect band gap QDs can have great potential for the hybrid cell in the future.

4. Conclusion

In conclusion, we successfully combine CdS QDs layer with GaAs solar cell to form a highly efficient hybrid solar cell. It is noticeable that the CdS QDs layer can significantly enhance power conversion efficiency under air mass 1.5 global illuminations. The main mechanism of the enhancement can be attributed to photon down-conversion and antireflection. Consequently, the overall power conversion efficiency is enhanced by 18.9% and 2.7%, when compared to the cell without CdS QDs layer (GaAs II) and the cell with conventional ARC (GaAs III), respectively. A further UV only test ascertains the enhancement of PCE can be constant at 1.22 times and CAFM shows the increased surface charges leading to the improvement of the fill factor by 30%. We believe this technology shall be a great candidate for next generation of highly efficient photovoltaic devices.

Acknowledgment

This work is funded by National Science Council in Taiwan under grant number NSC 99-2120-M-006-002 and NSC-99-2120-M-009-007. C. C. Lin would like to thank the financial support of National Science Council in Taiwan through the grant number: NSC101-3113-E-110-006-. The authors would also like to thank Prof. Shing-Chung Wang of NCTU for his help and support.